LETTERS

A quantum scattering interferometer

Russell A. Hart[1], Xinye Xu[1]†, Ronald Legere[1]† & Kurt Gibble[1]

The collision of two ultracold atoms results in a quantum mechanical superposition of the two possible outcomes: each atom continues without scattering, and each atom scatters as an outgoing spherical wave with an *s*-wave phase shift. The magnitude of the *s*-wave phase shift depends very sensitively on the interaction between the atoms. Quantum scattering and the underlying phase shifts are vitally important in many areas of contemporary atomic physics, including Bose–Einstein condensates[1–5], degenerate Fermi gases[6–9], frequency shifts in atomic clocks[10–12] and magnetically tuned Feshbach resonances[13]. Precise experimental measurements of quantum scattering phase shifts have not been possible because the number of scattered atoms depends on the *s*-wave phase shifts as well as the atomic density, which cannot be measured precisely. Here we demonstrate a scattering experiment in which the quantum scattering phase shifts of individual atoms are detected using a novel atom interferometer. By performing an atomic clock measurement using only the scattered part of each atom's wavefunction, we precisely measure the difference of the *s*-wave phase shifts for the two clock states in a density-independent manner. Our method will enable direct and precise measurements of ultracold atom–atom interactions, and may be used to place stringent limits on the time variations of fundamental constants[14].

In our experiment, we 'juggle' atoms[15] in an atomic fountain clock by launching two gaseous clouds of caesium atoms upwards in rapid succession (cloud 1 first, followed by cloud 2) by laser-cooling them in a frame that moves upwards at 2.5–3.4 m s^{-1}. Gravity slows the atoms and, after cloud 1 reaches its apogee and begins to fall, the two clouds pass through one another and the atoms collide. For a short time delay between launches, of the order of $\Delta t = 10$ ms, the relative velocity of the atoms is about $v_r = g\Delta t = 10\,\mathrm{cm\,s^{-1}}$ (where g is the acceleration due to gravity); this corresponds to a collision energy of $E = mv_r^2/4 = 40\,\mu\mathrm{K} \times k_B$ (where m is the atomic mass and k_B is Boltzmann's constant). The collision energy is much greater than the atoms' temperature of 250–500 nK. We prepare the atoms in cloud 1 in a pure $|F,m\rangle$ hyperfine state (for example, $|4,4\rangle$) and those in cloud 2 in one of the clock states ($|3,0\rangle$). Both clouds pass through a microwave (clock) cavity, which puts the atoms in cloud 2 in a coherent superposition of the two clock states, $|3,0\rangle$ and $|4,0\rangle$. The phase of this coherence precesses at the caesium clock frequency, $\nu \approx 9.2$ GHz (ref. 12). When the two clouds collide, the atoms scatter as illustrated in Fig. 1. The *s*-wave part of the atomic wavefunction in each clock state, $|3,0\rangle$ or $|4,0\rangle$, scatters off the atoms in cloud 1, acquiring an *s*-wave phase shift, δ_3 or δ_4. After scattering, the atoms fall back through the microwave cavity, which converts the phase difference between the clock coherence and the microwave field into a population difference of the clock states, which we detect. This population difference for the unscattered part of each atom's wavefunction yields the usual transition probability for a clock as a function of microwave frequency, known as Ramsey fringes[12] (red diamonds in Fig. 2a). Here we instead detect only the scattered part of each atom's wavefunction, for which the phase of the coherence is shifted by the difference of the *s*-wave phase shifts, $\Phi = \delta_3 - \delta_4$ (blue circles in Fig. 2a). In this way, we use atomic-clock interferometry to directly observe the difference of the *s*-wave phase shifts. To demonstrate this technique, we scatter the caesium clock states off $|4,4\rangle$ at $v_r = 9.92\,\mathrm{cm\,s^{-1}}$ and measure $\Phi = -0.141(8)$ rad.

To select a clock atom that scatters, we use the Doppler shift and a narrow two-photon Raman transition[15–17]. In Fig. 3, we show velocity distributions of the vertical velocity component (v_z) of cloud 2, prepared in $|3,0\rangle$, when it collides with $|4,4\rangle$ atoms in cloud 1. For the data in Fig. 3, the microwave pulses to the clock cavity are disabled so that cloud 2 is not prepared in a coherent superposition of the clock states. The velocity-selective probe pulse transfers atoms from $|3,0\rangle$ to $|4,0\rangle$ with a bandwidth of 1.4 cm s^{-1}, and we detect the number of atoms in $F = 4$. Before the probe pulse, we push the atoms in $F = 4$ from the fountain with a laser beam tuned to excite $F = 4$ atoms[15,17]. We push the $F = 4$ atoms either early, before cloud 1 enters the clock cavity, or late, right after both clouds return downward through the clock cavity. Early clearing gives the 'no-collisions' signal in Fig. 3a (violet), and late clearing allows the two clouds to collide before we clear cloud 1, giving the 'collisions' signal in Fig. 3a (aqua). In the magnified Fig. 3b, the difference between the 'collisions' and 'no-collisions' curves between $v_z = -5\,\mathrm{cm\,s^{-1}}$ and $2\,\mathrm{cm\,s^{-1}}$ represents scattered atoms (Fig. 3c). For both curves in Fig. 3a and b, we subtract the small backgrounds in Fig. 3d, obtained by inhibiting the preparation of cloud 2 in $|3,0\rangle$. To observe the Ramsey fringes of scattered atoms (blue circles in Fig. 2), we fix the probe velocity at $v_z = 0$ in Fig. 3c, which corresponds to 90° scattering, enable the microwave clock pulses, and then scan the frequency of the microwave clock pulses. The contributions to the Ramsey fringes at $v_z = 0$ from the

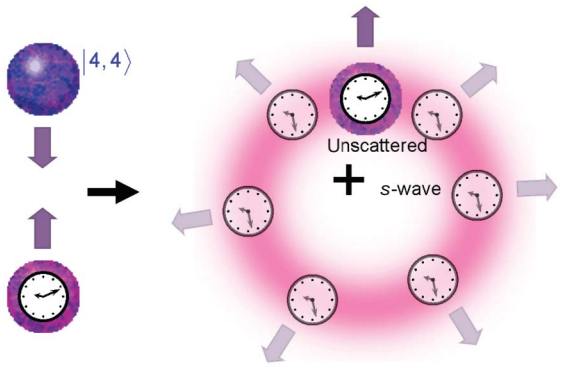

Figure 1 | Diagram of the experiment. Left, we collide an atom in a coherent superposition of the two caesium clock states (bottom) with a caesium atom in a pure $|F,m\rangle$ state, such as $|4,4\rangle$ (top). When the clock states scatter, they experience different *s*-wave phase shifts, shifting the phase of the clock coherence by the difference of the *s*-wave phase shifts. After the scattering (right), we directly observe the difference of the *s*-wave phase shifts by detecting only the scattered part of each clock atom's wavefunction.

[1]Department of Physics, The Pennsylvania State University, University Park, Pennsylvania 16802, USA. †Present addresses: Department of Physics, East China Normal University, Shanghai 200062, China (X.X.); MIT Lincoln Laboratory, Lexington, Massachusetts 02420, USA (R.L.).

'no-collisions' and backgrounds are small, with phase shifts consistent with 0 (Fig. 2b and c). For this first demonstration, we choose 90° scattering to avoid contributions from *p*-waves.

These measurements are qualitatively different from the usual cold-collisions frequency shift in an operating atomic clock. The usual frequency shift arises from a collision rate which gives the rate at which the phase of the coherence is shifted. The usual frequency shift is due to the quantum-mechanical interference in the forward direction between the unscattered and scattered parts of each atom[18,19] and is proportional to density[10–12]. Here, the Ramsey fringes for the atoms that scatter have a phase shift (which is independent of density) instead of a frequency shift, because the phase of the coherence of the scattered part of each atom experiences both *s*-wave phase shifts, δ_3 and δ_4. To demonstrate the qualitative differences, we show in Fig. 4a the phase shift as a function of the free precession time T between the two microwave pulses for $T = 0.115$ s to 0.450 s. We increase the free precession time by increasing the launch velocity of both clouds, so that their apogees above the clock cavity are higher[12]. The phase shift is independent of T. It is clearly inconsistent with a frequency shift, for which the phase shift would increase linearly with T (dashed line in Fig. 4a). Further, the magnitudes of the effects are very different. The largest cold-collision frequency shift that has been observed in a clock is −5.5 mHz (ref. 10). Here, for $T = 0.115$ s, a phase shift of $\Phi = -0.141$ rad corresponds to a frequency shift of −200 mHz.

A key feature of this technique is that this difference of quantum scattering phase shifts is independent of the atomic density, to lowest order (Fig. 4b). Many experiments have probed a wide variety of scattering effects, including velocity redistribution[17,20], frequency shifts[10,11] and inelastic losses[21]. Each of these effects is given by a rate $nv_r\sigma$, where n is the atomic density and σ is the cross-section for the process. As the best measurements of the density of cold atoms do not achieve even 1% accuracy[22,23], it is generally not possible to precisely determine atomic scattering phase shifts and the atom–atom interactions from these measurements. Indeed for caesium, many scattering results appeared thoroughly inconsistent until the spectroscopic observation of many Feshbach resonances[24], combined with a theoretical analysis, determined the caesium interaction properties[25]. Here, although the number of scattered atoms and the amplitude of the Ramsey fringes are proportional to the density of cloud 1 (Fig. 4b inset), the phase shift is independent of the atomic density and therefore can utilize the high accuracy available with atomic clock techniques. In this first measurement, our statistical uncertainty is 6% (of even a relatively small difference of *s*-wave phase shifts), compared to typical density uncertainties of a factor of

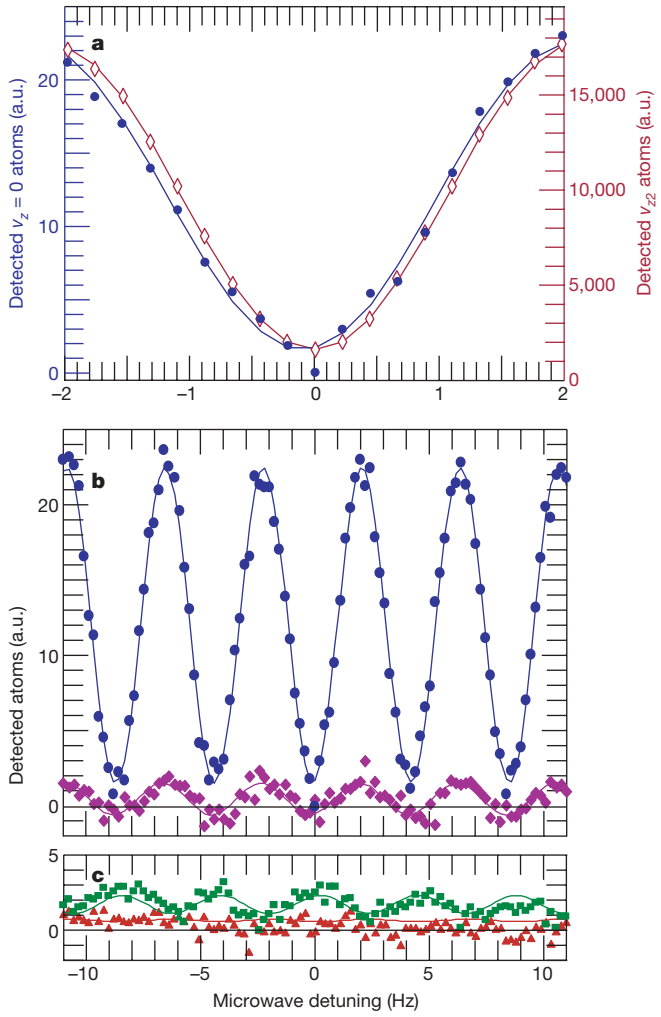

Figure 2 | Ramsey fringes for scattered and unscattered atoms. **a**, The central Ramsey fringe for clock atoms that have *s*-wave scattered from $|4,4\rangle$ atoms at 90° ($v_z = 0$, blue circles) with $v_r = 9.92\,\mathrm{cm\,s^{-1}}$. The reference Ramsey fringe is from the unscattered clock atoms (v_{z2}, maroon diamonds). The fringes for the scattered atoms have a phase shift of −0.141 rad, which is the difference of the *s*-wave phase shifts. a.u., arbitrary units. **b**, The entire Ramsey pattern for scattered atoms at $v_z = 0$ (blue circles) and for 'no-collisions' (violet diamonds) as in Fig. 3. **c**, The background Ramsey fringes as in Fig. 3 for 'collisions' (green squares) and 'no-collisions' (red triangles). For these data, the difference of the *s*-wave phase shifts for the clock states scattering off $|4,4\rangle$ is relatively small, $\Phi = -0.141(12)$ rad. Each circle represents the average of four differences of four measurements, requiring 16 cycles of the atomic fountain. The central Ramsey fringe is a minimum because the atoms begin in the $|3,0\rangle$ clock state and we detect the final number in $|3,0\rangle$. In **a**, there are nearly 1,000 times more unscattered atoms (maroon diamonds) than detected scattered atoms (blue circles).

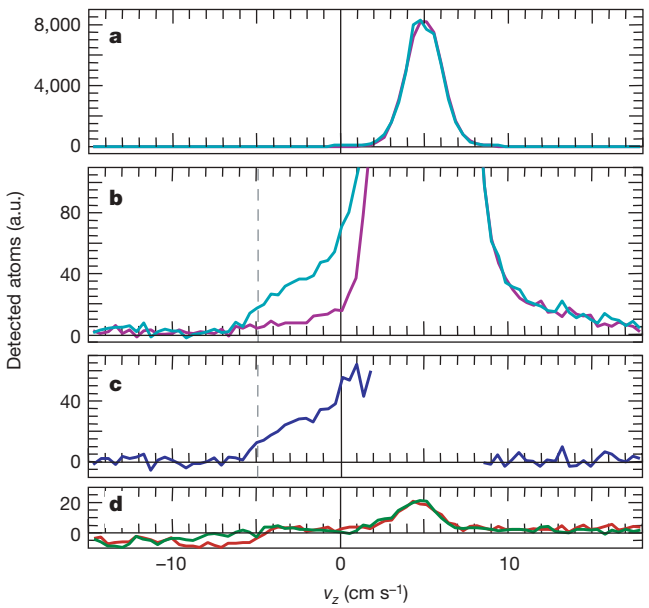

Figure 3 | Velocity distribution of clock atoms. Cloud 2 is prepared in $|3,0\rangle$ and cloud 1 in $|4,4\rangle$, with $v_r = 9.92\,\mathrm{cm\,s^{-1}}$. **a**, The aqua (violet) curves show the velocity distribution of cloud 2 for 'collisions' ('no-collisions') when we clear cloud 1 from the fountain late (early). **b**, Magnification of **a** by a factor of 100. In this centre-of-mass frame, the most probable vertical velocity component for cloud 1 is $v_{z1} = -4.96\,\mathrm{cm\,s^{-1}}$ (dashed line) and $v_{z2} = 4.96\,\mathrm{cm\,s^{-1}}$ for cloud 2. **c**, The difference between the 'collisions' and 'no-collisions' curves. This represents scattered atoms, which are visible between $v_z = -5\,\mathrm{cm\,s^{-1}}$ and $2\,\mathrm{cm\,s^{-1}}$. **d**, Background for 'collisions' (green) and 'no-collisions' (red). The Ramsey fringes in Fig. 2 (blue, violet, green, and red) are taken at $v_z = 0$ here on the curve of the same colour. The Ramsey fringes in Fig. 2 for unscattered atoms (maroon diamonds) are taken at v_{z2}. About 0.1% of the atoms scatter into the $1.4\,\mathrm{cm\,s^{-1}}$ detected velocity width at 90°.

two. Although measurements of differential cross-sections also yield density-independent phase shift differences[15,26,27], potential systematic errors that depend on the scattering angle limit the precision. Future improvements of our precision by orders of magnitude are expected.

At low energies, the atom–atom interactions are described by the *s*-wave scattering length, *a*. The scattering length is the low-temperature limit of $-\delta/k$ (where $k = \pi m v_r/h$ is the atomic wave vector and h is Planck's constant). Therefore, direct measurements of the difference of *s*-wave phase shifts can directly give precise differences of *s*-wave scattering lengths[5]. Using $\delta = -ka$, our current precision would translate to a scattering length difference uncertainty of ± 0.7 Å, comparable to the current uncertainty of the caesium triplet scattering length, $a = 1291.2(5)$ Å (ref. 25). A future accuracy of 100 μrad for Φ yields ± 0.009 Å, or 7 p.p.m. However, the caesium triplet scattering length is so large that $ka > 1$ for even $E = 1\ \mu\mathrm{K} \times k_B$. Therefore, our sensitivity to the caesium interatomic potentials at these energies is not so simple, and theoretical work is required to establish the sensitivity. Preliminary work has shown a sensitivity to scattering lengths of 1–100 p.p.m. for a measurement accuracy of 100 μrad (ref. 19). Chin and Flambaum[14] have recently suggested that highly sensitive measurements of scattering lengths near Feshbach resonances will set stringent limits on the time variation of the electron/proton mass ratio, a fundamental constant of physics. Near a Feshbach resonance, the phase shift in Fig. 2a has a resonant structure and varies by π. Our technique can accurately measure the phase shift throughout a resonance.

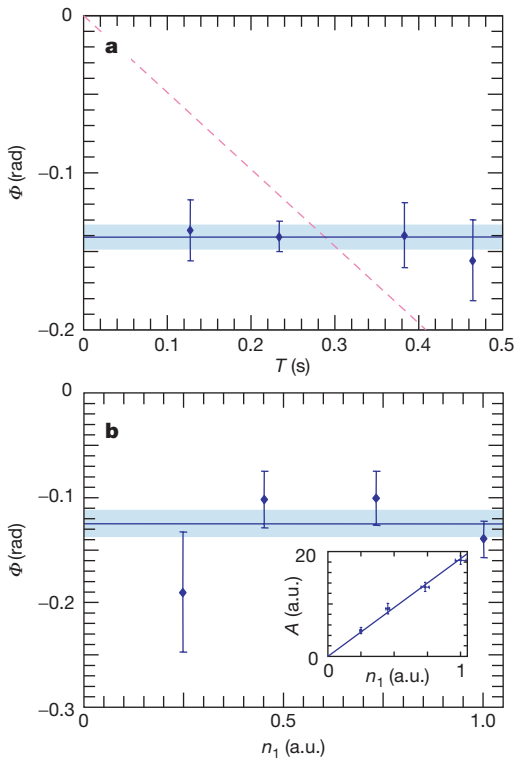

Figure 4 | The *s*-wave phase shift of scattered atoms. a, The phase shift Φ versus the free precession time T between the two microwave field interactions. The phase shift is independent of T, as opposed to being proportional to T as it is for a frequency shift (dashed line). We increase T by increasing the launch velocity in the fountain. The best fit to all the data is $\Phi = -0.141(8)$. **b**, The phase shift and Ramsey fringe amplitude, A, (inset) versus the atom density of cloud 1, n_1. The phase shift is independent of the density rather than proportional to it; in contrast, the usual cold-collision frequency shift in clocks is proportional to the density. As expected, the Ramsey fringe amplitude is proportional to the density of atoms in cloud 1. The error bars and bands represent standard errors.

We have demonstrated a fundamentally new scattering method that directly observes the phase shift of an atomic coherence due to quantum scattering. We use an atom interferometer in an atomic clock to accurately measure the difference of *s*-wave phase shifts. The technique is quite general; for any atom with a magnetic-field-insensitive transition, a variety of scattering channels can be explored with high accuracy. For caesium, any of the 16 hyperfine states can be studied as a function of collision energy and magnetic field for *s* waves, and for higher partial angular-momentum waves such as *p*, *d* and so on. The technique offers direct and unambiguous differences of quantum scattering phase shifts, and stringently probes ultracold atom–atom interactions.

METHODS

Juggling atomic fountain clock. Here we describe the changes to our juggling fountain, which is based on a double magneto-optic trap (MOT)[15,17]. We cool and optically pump each cloud of atoms after they are launched from the ultra-high-vacuum MOT in a three-dimensional moving-frame optical lattice with degenerate Raman-sideband cooling[28,29]. This optically pumps the atoms into the $|3,3\rangle$ state and cools them to a temperature of typically 500 nK for cloud 1, and 250 nK for cloud 2. Instead of launching both clouds with the same velocity, we launch cloud 1 with a slightly larger velocity than cloud 2 so that the two clouds collide after their apogees. The two clouds finish passing through one another just before they return downward through the microwave cavity. This has two advantages: (1) the two clouds are further separated at launch so that more of the atoms in cloud 1 survive the launch of cloud 2, and (2) it shortens the time between the collisions and the detection. After the clouds collide, the atoms spread out spherically with a velocity of $v_r/2 \approx 5\ \mathrm{cm\,s^{-1}}$. For the scattered atoms to be detected, they must pass through the 1.8 cm cavity apertures and be illuminated by the 2-cm-diameter detection laser beam. The highest collision rate occurs when the two cloud centres coincide, and the time from this point until we detect the scattered atoms is typically 0.13 s, so that the scattered cloud of these atoms spreads to a diameter of 1.3 cm.

We have added six 9.2-GHz microwave cavities to our juggling fountain to drive microwave transitions. The cavities used for the clock pulses and the state preparation are TE_{011} cylindrical cavities, dielectrically loaded with fused silica to reduce their size. The state-preparation cavities have 12-mm-diameter apertures in their endcaps, through which the atoms pass, and those for the clock cavity are 18 mm in diameter. Above the clock cavity, there is a $TE_{0,1,13}$ cavity that we use to probe the magnetic field[11], which is maintained near 15 mG. We pulse the microwaves to the clock cavity and, because of some leakage to the $TE_{0,1,13}$ cavity, we pulse the appropriate power and phase to it. We adjust the amplitude and phase so that the phase of the microwave field in the clock cavity is constant to less than 0.015 rad up to 7.4 mm above the centre of the clock cavity. In addition, we apply the 5-ms-long pulses when the atoms are centred in the clock cavity. In a future version, we will eliminate this leakage.

For the final state detection after the atoms pass downward through the clock cavity, we insert an aperture in the detection laser beam to limit the contributions from the unscattered atoms in clouds 1 and 2. With a vertical aperture height of the order of 1 cm, the background Ramsey fringes (violet, red and green curves in Fig. 2) are small. With no aperture, the background Ramsey fringes in Fig. 2 have amplitudes twice as large as the amplitude for scattered atoms, and still give the same phase shift.

State preparation. Both clouds of atoms are launched from the optical lattice in the $|3,3\rangle$ state and then pass through four microwave state-preparation cavities. A typical sequence for $T = 233$ ms follows (for other launch velocities, the order of the pulses may be slightly different). To minimize backgrounds, we purify the optical pumping of cloud 1 by transferring any residual atoms in $|3,1\rangle$ and $|3,2\rangle$ to the $F = 4$ hyperfine level with composite π pulses[30] in the first state-preparation cavity and pulsing a laser beam that pushes $F = 4$ atoms from the fountain. This is repeated in the second state-preparation cavity for $|3,-1\rangle$ and $|3,0\rangle$. After this, cloud 2 enters the first cavity and, as it travels through the first three cavities, a composite π pulse in each cavity transfers the atoms in $|3,3\rangle$ to $|4,3\rangle$ to $|3,2\rangle$, and finally to $|4,1\rangle$. In the middle of this sequence, cloud 1 is in the third cavity and we transfer those atoms from $|3,3\rangle$ to $|4,4\rangle$. After both clouds leave the cavities, we apply a laser pulse to repump any atoms left in $F = 3$. A stimulated-Raman transition then velocity-selectively transfers the atoms in cloud 2 from $|4,1\rangle$ to $|3,0\rangle$ before they enter the clock microwave cavity. The peak densities of cloud 1 (2) at launch are 6×10^9 $(1.2 \times 10^9)\ \mathrm{cm^{-3}}$, which we measure by observing collisions within one cloud[17] between $|3,0\rangle$ and $|4,0\rangle$, for which the triplet scattering length[25] gives a cross-section near the unitary limit. The number of atoms in cloud 1 and cloud 2 is about 1.6×10^9 and 3×10^8, respectively.

Received 5 January; accepted 8 February 2007.

1. Hall, D. S., Matthews, M. R., Ensher, J. R., Wieman, C. E. & Cornell, E. A. Dynamics of component separation in a binary mixture of Bose-Einstein condensates. *Phys. Rev. Lett.* **81,** 1539–1542 (1998).
2. Stenger, J. *et al.* Spin domains in ground-state Bose–Einstein condensates. *Nature* **396,** 345–348 (1998).
3. Khaykovich, L. *et al.* Formation of a matter-wave bright soliton. *Science* **296,** 1290–1293 (2002).
4. Strecker, K. E., Partridge, G. B., Truscott, A. G. & Hulet, R. G. Formation and propagation of matter-wave soliton trains. *Nature* **417,** 150–153 (2002).
5. Widera, A. *et al.* Precision measurement of spin-dependent interaction strengths for spin-1 and spin-2 ^{87}Rb atoms. *New J. Phys.* **8,** 152 (2006).
6. DeMarco, B. & Jin, D. S. Onset of Fermi degeneracy in a trapped atomic gas. *Science* **285,** 1703–1706 (1999).
7. Modugno, G. *et al.* Collapse of a degenerate Fermi gas. *Science* **297,** 2240–2243 (2002).
8. O'Hara, K. M., Hemmer, S. L., Gehm, M. E., Granade, S. R. & Thomas, J. E. Observation of a strongly interacting degenerate Fermi gas of atoms. *Science* **298,** 2179–2182 (2002).
9. Gupta, S. *et al.* Radio-frequency spectroscopy of ultracold fermions. *Science* **300,** 1723–1726 (2003).
10. Gibble, K. & Chu, S. Laser-cooled Cs frequency standard and a measurement of the frequency shift due to ultracold collisions. *Phys. Rev. Lett.* **70,** 1771–1774 (1993).
11. Fertig, C. & Gibble, K. Measurement and cancellation of the cold collision shift in an ^{87}Rb fountain clock. *Phys. Rev. Lett.* **85,** 1622–1625 (2000).
12. Wynands, R. & Weyers, S. Atomic fountain clocks. *Metrologia* **42,** S64–S79 (2005).
13. Inouye, S. *et al.* Observation of Feshbach resonances in a Bose–Einstein condensate. *Nature* **392,** 151–154 (1998).
14. Chin, C. & Flambaum, V. V. Enhanced sensitivity to fundamental constants in ultracold atomic and molecular systems near Feshbach resonances. *Phys. Rev. Lett.* **96,** 230801 (2006).
15. Legere, R. & Gibble, K. Quantum scattering in a juggling atomic fountain. *Phys. Rev. Lett.* **81,** 5780–5783 (1998).
16. Kasevich, M. *et al.* Atomic velocity selection using stimulated Raman transitions. *Phys. Rev. Lett.* **66,** 2297–2300 (1991).
17. Gibble, K., Chang, S. & Legere, R. Direct observation of s-wave atomic collisions. *Phys. Rev. Lett.* **75,** 2666–2669 (1995).
18. Legere, R. J. *Quantum Scattering in a Juggling Atomic Fountain*. PhD thesis, Yale Univ. (1999).
19. Kokkelmans, S. J. J. M. F. *Interacting Atoms in Clocks and Condensates*. PhD thesis, Univ. Eindhoven (2000).
20. Monroe, C. R., Cornell, E. A., Sackett, C. A., Myatt, C. J. & Wieman, C. E. Measurement of Cs-Cs elastic scattering at T = 30 μK. *Phys. Rev. Lett.* **70,** 414–417 (1993).
21. Myatt, C. J., Burt, E. A., Ghrist, R. W., Cornell, E. A. & Wieman, C. E. Production of two overlapping Bose-Einstein condensates by sympathetic cooling. *Phys. Rev. Lett.* **78,** 586–589 (1997).
22. Ensher, J. R., Jin, D. S., Matthews, M. R., Wieman, C. E. & Cornell, E. A. Bose-Einstein condensation in a dilute gas: Measurement of energy and ground-state occupation. *Phys. Rev. Lett.* **77,** 4984–4987 (1996).
23. DePue, M. T., McCormick, C., Winoto, S. L., Oliver, S. & Weiss, D. S. Unity occupation of sites in a 3D optical lattice. *Phys. Rev. Lett.* **82,** 2262–2265 (1999).
24. Chin, C., Vuletic, V., Kerman, A. J. & Chu, S. High resolution Feshbach spectroscopy of cesium. *Phys. Rev. Lett.* **85,** 2717–2720 (2000).
25. Chin, C. *et al.* Precision Feshbach spectroscopy of ultracold Cs_2. *Phys. Rev. A* **70,** 032701 (2004).
26. Thomas, N. R., Kjærgaard, N., Julienne, P. S. & Wilson, A. C. Imaging of s and d partial-wave interference in quantum scattering of identical bosonic atoms. *Phys. Rev. Lett.* **93,** 173201 (2004).
27. Buggle, Ch, Léonard, J., von Klitzing, W. & Walraven, J. T. M. Interferometric determination of the s and d-wave scattering amplitudes in ^{87}Rb. *Phys. Rev. Lett.* **93,** 173202 (2004).
28. Hamann, S. E. *et al.* Resolved-sideband Raman cooling to the ground state of an optical lattice. *Phys. Rev. Lett.* **80,** 4149–4152 (1998).
29. Treutlein, P., Chung, K. Y. & Chu, S. High-brightness atom source for atomic fountains. *Phys. Rev. A* **63,** 051401(R) (2001).
30. Levitt, M. H. Composite pulses. *Prog. Nucl. Magn. Reson. Spectrosc.* **18,** 61–122 (1986).

Acknowledgements We acknowledge discussions with B. Verhaar and S. Kokkelmans and contributions from R. Li. This work was supported by NASA, NSF, ONR and Penn State University.

Author Information Reprints and permissions information is available at www.nature.com/reprints. The authors declare no competing financial interests. Correspondence and requests for materials should be addressed to K.G. (kgibble@psu.edu).